



OPEN

Apelin promotes blood and lymph vessel formation and the growth of melanoma lung metastasis

Judit Berta¹, Szilvia Török¹, Júlia Tárnoki-Zách², Orsolya Drozdovszky¹, József Tóvári³, Sándor Paku⁴, Ildikó Kovács¹, András Czirók^{2,5,6}, Bernard Masri⁷, Zsolt Megyesfalvi^{1,8,9}, Henriett Oskolás¹⁰, Johan Malm¹¹, Christian Ingvar¹², György Markó-Varga¹⁰, Balázs Döme^{1,8,9,13}✉ & Viktória László^{1,8,13}✉

Apelin, a ligand of the APJ receptor, is overexpressed in several human cancers and plays an important role in tumor angiogenesis and growth in various experimental systems. We investigated the role of apelin signaling in the malignant behavior of cutaneous melanoma. Murine B16 and human A375 melanoma cell lines were stably transfected with apelin encoding or control vectors. Apelin overexpression significantly increased melanoma cell migration and invasion *in vitro*, but it had no impact on its proliferation. In our *in vivo* experiments, apelin significantly increased the number and size of lung metastases of murine melanoma cells. Melanoma cell proliferation rates and lymph and blood microvessel densities were significantly higher in the apelin-overexpressing pulmonary metastases. APJ inhibition by the competitive APJ antagonist MM54 significantly attenuated the *in vivo* pro-tumorigenic effects of apelin. Additionally, we detected significantly elevated circulating apelin and VEGF levels in patients with melanoma compared to healthy controls. Our results show that apelin promotes blood and lymphatic vascularization and the growth of pulmonary metastases of skin melanoma. Further studies are warranted to validate apelin signaling as a new potential therapeutic target in this malignancy.

Abbreviations

MEK	Mitogen-activated protein kinase kinase
VEGF	Vascular endothelial growth factor
RT-qPCR	Reverse transcription-quantitative polymerase chain reaction
ECM	Extracellular matrix
BrdU	5-Bromo-2'-deoxyuridine
GEPIA2	Gene expression profiling interactive analysis 2
TIMER 2.0	Tumor immune estimation resource 2.0
SRB	Sulforhodamine B
Erk	Extracellular signal-regulated kinase
MMP-1	Matrix metalloproteinase-1
MMP-9	Matrix metalloproteinase-9
IL-2	Interleukin-2

¹Department of Tumor Biology, National Korányi Institute of Pulmonology, Budapest, Hungary. ²Department of Biological Physics, Eötvös University, Budapest, Hungary. ³Department of Experimental Pharmacology, National Institute of Oncology, Budapest, Hungary. ⁴1st Department of Pathology and Experimental Cancer Research, Semmelweis University, Budapest, Hungary. ⁵Department of Anatomy and Cell Biology, Medical Center, University of Kansas, Kansas City, KS, USA. ⁶University of Kansas Cancer Center, Kansas City, KS, USA. ⁷Department of Endocrinology, Metabolism and Diabetes, Institute Cochin, INSERM U1016, CNRS UMR8104, Université de Paris, Paris, France. ⁸Translational Thoracic Oncology Laboratory, Department of Thoracic Surgery, Comprehensive Cancer Center Vienna, Medical University of Vienna, Vienna, Austria. ⁹Department of Thoracic Surgery, National Institute of Oncology and Semmelweis University, Budapest, Hungary. ¹⁰Clinical Protein Science and Imaging, Biomedical Center, Department of Biomedical Engineering, Lund University, Lund, Sweden. ¹¹Department of Translational Medicine, Section for Clinical Chemistry, Lund University, Malmö, Sweden. ¹²Department of Surgery, Skåne University Hospital, Lund, Sweden. ¹³These authors contributed equally: Balázs Döme and Viktória László. ✉email: balazs.dome@meduniwien.ac.at; viktoria.laszlo@meduniwien.ac.at

IL-6	Interleukin-6
EDTA	Ethylenediaminetetraacetic acid
ELISA	Enzyme-linked immunosorbent assay
DMEM	Dulbecco's modified Eagle's medium
FBS	Fetal bovine serum
PIV	Particle image velocimetry
PBS	Phosphate buffered saline
IHC	Immunohistochemical staining
BSA	Bovine serum albumin
LYVE-1	Lymphatic vessel endothelial receptor 1

Cutaneous melanoma is the most aggressive form of skin cancers. When metastasized, the prognosis is poor with a 5-year survival rate of patients with distant metastases of only 5–10%. In patients with advanced stage melanoma, both conventional chemotherapy and radiotherapy have been largely ineffective, but during the last 10 years BRAF and mitogen-activated protein kinase kinase (MEK) inhibitors and checkpoint inhibitors have changed the scene with a 5-year survival of up to 50% in disseminated disease^{1–9}. Still there is a need to find novel targets in the treatment of this disease.

Apelin, an endogenous ligand of the G-protein coupled APJ receptor was first isolated from bovine stomach extracts in 1998¹⁰. Apelin peptide is expressed in the central nervous system and in various peripheral tissues, including the heart, lung, and mammary glands¹¹. Besides, it circulates in the plasma at low, picomolar concentrations¹². The apelinergic system has various physiological and pathophysiological roles^{12–14}. Apelin was reported to stimulate angiogenesis in various non-tumorous in vitro and in vivo systems^{15,16}. During embryonic development, APJ receptor expression is largely restricted to the endothelial cells of the developing vascular system, and apelin/APJ are highly expressed in the adult vessel walls as well^{17,18}.

Several studies demonstrated that apelin also plays a role in tumor angiogenesis and can enhance the growth of different tumors (e.g. glioblastoma multiforme, mammary carcinoma and non-small cell lung cancer)^{19–21}. The apelin-APJ system was demonstrated to induce the morphological and functional maturation of blood vessels in mouse melanoma, colon cancer, and human prostate cancer xenografts²². Apelin blockage inhibited tumor growth and normalized blood vessels by reduced capillary leakage and tissue hypoxia and maintained pericyte coverage in vivo in mammary and breast cancer mouse models²³. Moreover, it was demonstrated that apelin and vascular endothelial growth factor (VEGF) can concomitantly regulate the key angiogenesis-related pathways²³. It has also been reported that, besides its pro-angiogenic effect, apelin can also induce the growth of lymphatic vessels. Apelin was reported to promote the migration and capillary-like tube formation of lymphatic endothelial cells, and it increased their 3D growth as well. Moreover, apelin overexpression in mouse melanoma cells promoted in vivo tumor growth and increased intratumoral lymphangiogenesis and lymph node metastasis²⁴. These results suggest that apelin plays a role in both angio- and lymphangiogenesis.

In line with the abovementioned observations, apelin was reported to be overexpressed in several human cancers and, moreover, in many tumor types its high tumor and blood levels were associated with unfavorable prognosis^{20,21,25–31}. Apelin overexpression was reported in muscle-invasive bladder cancer and hepatocellular carcinoma. Accordingly, high level of apelin indicates a poor prognosis in these tumor types^{32–34}. Apelin up-regulation is significantly associated with advanced pathologic stage and metastasis in patients with prostate cancer³⁰. Hypoxia-induced apelin is a negative prognostic factor in oral squamous cell carcinoma²⁷. Apelin is significantly upregulated both in low and high grade gliomas³⁵ and also in gastroesophageal cancer^{25,26}. Circulating apelin levels are significantly elevated in patients with breast, head and neck and colorectal cancers^{36–38}.

Several papers studied the exact role of apelin in primary tumors and tumor angiogenesis, but there is a lack of research related to the role of apelin in the disseminating process. Only a very recent paper investigated the role of APJ signaling in ovarian cancer progression and metastasis. These authors showed that overexpression of APJ supports the pro-metastatic phenotype in ovarian cancer cells in vitro, and the intraperitoneal metastasis of these cells in vivo³⁹.

In malignant melanoma the lung is one of the most frequent site of metastatic growth^{40,41}. Consequently, in this study we focus on the role of the (lymph)angiogenic apelin molecule in pulmonary metastases of malignant melanoma.

Results

Apelin promotes melanoma cell migration and invasion in vitro. APJ receptor expression was shown in some cancer cell lines^{42,43}. To ensure whether apelin overexpression could be APJ dependent, we performed immunocytochemical and western blot analysis, and demonstrated the presence of APJ protein in apelin overexpressing and control B16 and A375 cells (Supp Fig. 1A–E). The overexpression of apelin in melanoma cells was validated by reverse transcription-quantitative polymerase chain reaction (RT-qPCR). Apelin showed a 303-fold and 290-fold overexpression in B16 Ap and A375 Ap cells, respectively, compared to their control vector-transfected counterparts ($p < 0.05$; Supp Fig. 1G). Previous reports have shown that apelin stimulates migration in various normal and malignant cell types, including vascular smooth muscle cells⁴⁴, retinal pigment epithelial cells⁴⁵ lymphatic endothelial cells²⁴ and oral²⁷ and gastric cancer cell lines³⁶. In our experiments, apelin overexpression significantly enhanced the migration of B16 and A375 cells independently of cell density (90 vs. 30 vs. 10 cells/mm²) both on non-coated and on collagen I-coated surfaces ($p < 0.0001$; Fig. 1A–B). Supplemental Movies 1 (SM1) demonstrate the movement of B16 (SM1A) or A375 (SM1B) melanoma cells at 90 cells/mm² density on collagen-I surface.

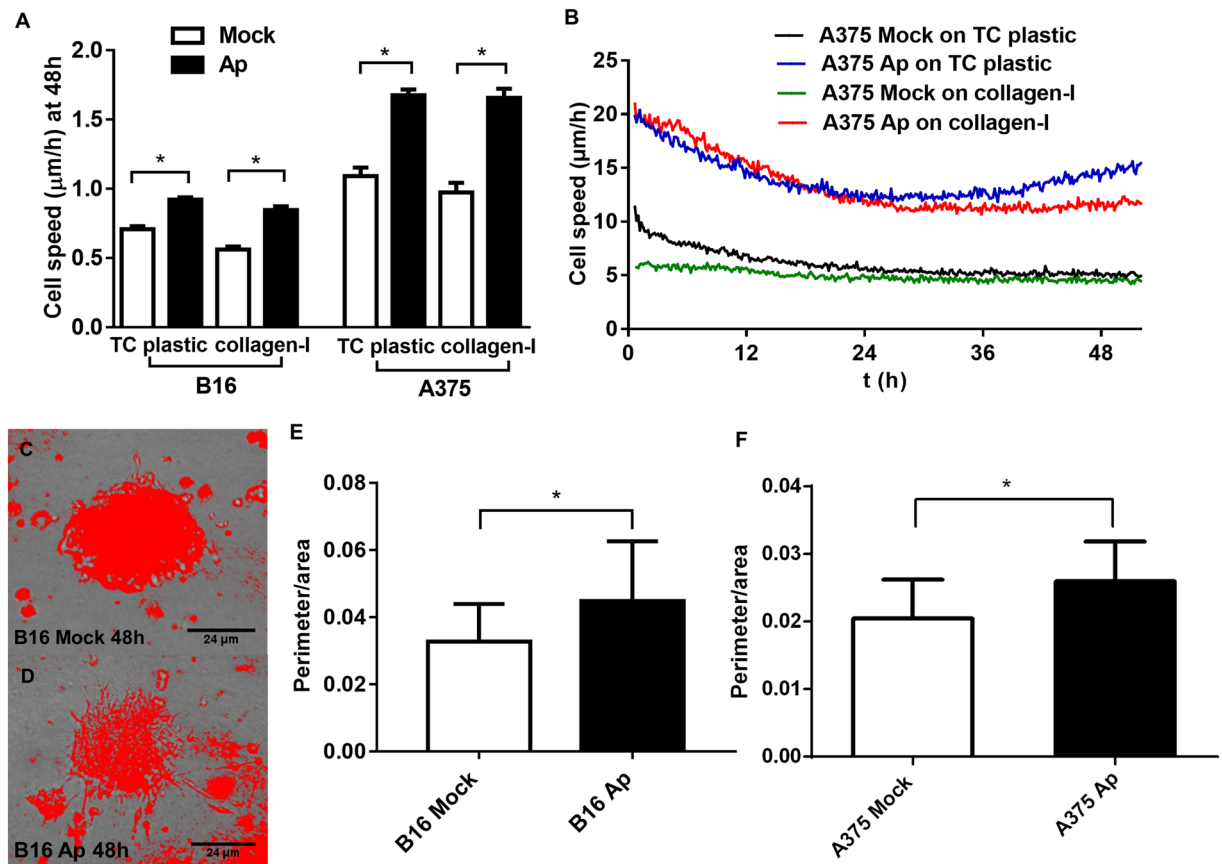


Figure 1. Apelin overexpression enhances the migratory activity and invasive capacity of melanoma cell lines. (A) Overexpression of apelin in B16 and A375 melanoma cells increased 2D motility independently of cell density (10/30/90 cell/mm²) and surface (TC plastic vs. collagen I). Columns show the average cell speed in two experiments with three cell densities at 48 h +/− SEM. (B) Representative curves of time-dependent average speed demonstrating increased cell motility in apelin-overexpressing A375 cells regardless of the surface (non-precoated vs. collagen I coated) at 90 cell/mm² cell density. (C–F) Representative images and quantification of tumor cell invasion. Apelin overexpression significantly increased the perimeter/area ratio of spheroids compared to spheroids formed by cells transfected with control vector. Columns, mean for three experiments; bars, standard error of the mean. **p* < 0.05.

The 3D tumor spheroid invasion assay is a useful method to assess tumor cell invasion in vitro because the expression of proteins regulating tumor cell invasion may differ between 2 and 3D conditions. When spheroid aggregates are placed into collagen 1 type gel as extracellular matrix (ECM) substrate, the tumor cells spread out from the spheroid body and extend into the extracellular-like environment^{46,47}. In our experiments, apelin overexpression increased the perimeter/area ratio of B16 or A375 spheroids (*p* < 0.005; Fig. 1C–F). Moreover, when the single melanoma cells were let to form spheroids in a collagen gel, tumor cells more visibly spread out from the spheroids in case of apelin overexpressing melanoma cells compared to the cells transfected with control vector. Supplemental Movies 2 (SM2) show the apelin overexpressing B16 (SM2A) or A375 (SM2B) cells compared to control cells, respectively.

Interestingly, when the effect of apelin overexpression was investigated in a sulforhodamine B (SRB) assay, we found that apelin had no impact on the in vitro proliferation of B16 or A375 cells, regardless of the initial cell density (*p* > 0.05; Supp Fig. 2).

Accelerated pulmonary metastasis of apelin-overexpressing melanoma cells is fueled by increased tumor cell proliferation and enhanced blood and lymph vessel formation.

In order to investigate the effect of apelin overexpression on lung metastases in a mouse model of melanoma, apelin-overexpressing and control B16 cells were injected intravenously into C57Bl/6 mice. Mice injected with apelin-overexpressing melanoma cells were also treated with the APJ antagonist MM54 or saline, twice a week, intraperitoneally. Lungs were removed 3 weeks after tumor cell injection, and the metastases were counted and measured with ocular micrometer (Fig. 2A–E). Apelin overexpression significantly increased the number and area of lung metastases (vs. B16 Mock, *p* < 0.0001; Fig. 2D–E). Inhibition of APJ signaling by MM54 significantly decreased the size (*p* = 0.0047; Fig. 2E), but not the number of lung metastases formed by apelin-overexpressing cells (*p* = 0.2055; Fig. 2D). Histological analysis of the tumors revealed that blood and lymph vessel densities were higher in B16 Ap metastases (vs. B16 Mock metastases; *p* < 0.05) and, furthermore, that MM54 inhibited blood vessel formation significantly (*p* < 0.05; Fig. 3A–H). In line with these findings, the number of BrdU posi-

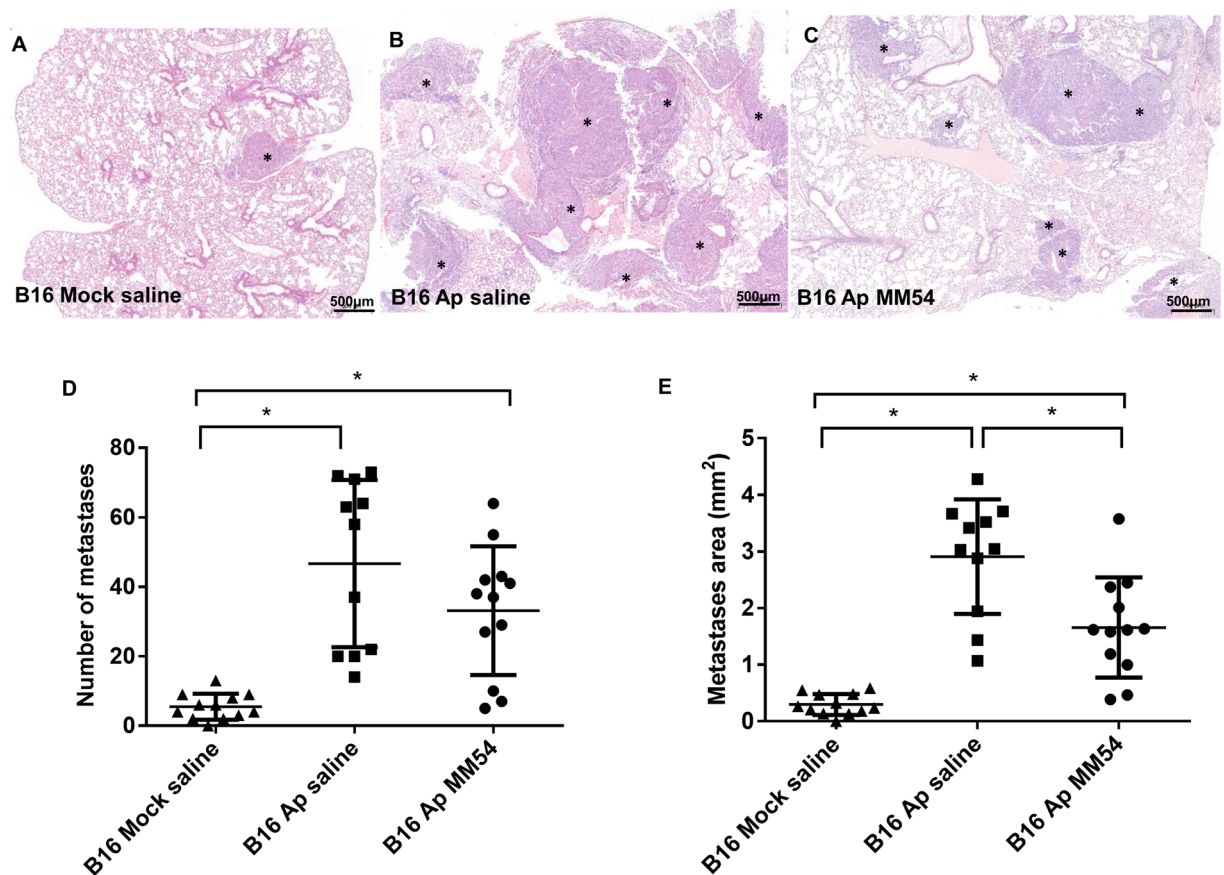


Figure 2. The effect of apelin overexpression and inhibition on the growth of experimental lung metastases. (A–C) Histological demonstration of lung metastases formed in the B16 Mock saline (A), B16 Ap saline (B) and B16 Ap MM54 (C) groups. Asterisks show the colony of the B16 Mock (A) or B16 Ap (B,C) melanoma cells in the lung. (D,E) Apelin overexpression significantly enhanced the number (D) and area (E) of B16 Ap lung metastases compared to the metastases of B16 Mock cells. Furthermore, the APJ antagonist MM54 had no impact on the number of metastases (D), but it significantly decreased the area of lung metastases formed by B16 Ap cells (E). * $p < 0.05$.

tive cells was also significantly increased in the B16 Ap metastases (vs. B16 Mock tumors; $p < 0.0001$) and MM54 decreased significantly the number of proliferating cells in apelin-overexpressing lung metastases, compared to apelin-overexpressing metastases treated with saline ($p < 0.0001$; Fig. 4A–D).

Apelin and VEGF plasma levels are elevated in melanoma patients. Next, we studied the clinical relevance of our observations in preclinical models of murine and human melanoma. It has been reported that patients with different types of tumors had higher circulating apelin levels compared to healthy controls^{26,36–38,48}. In line with these findings, we investigated the circulating apelin levels in patients with melanoma ($n = 40$) compared the healthy individuals ($n = 21$). Clinical characteristics of patients with melanoma and healthy controls are presented in Table 1. We studied the relation of apelin level and patients' age, but we could not see any correlation between these data (data not shown). In patients with melanoma, the following co-morbidities were also studied, as they might influence the circulating apelin levels: arterial hypertension, cardiovascular diseases, diabetes, asthma, inflammatory diseases, renal diseases^{28,49–53}. Table 1 shows the percentages of these co-morbidities in the patient cohort, some of them had more than one co-morbidities. We found that they have no significant impact on the circulating apelin levels of patients (data not shown). The healthy individuals had no cardiovascular or pulmonary disease; and they were checked 2 times/year for 5 years. In addition, 20 health blood biomarkers have been screened for hematological and inflammatory markers and other routine biomarkers, reflecting the health status of the participant. Studying the circulating apelin levels, we found that the plasma levels of apelin were significantly elevated in patients with melanoma (vs. healthy controls, 1.4590 ± 0.2676 ng/ml vs. 0.7704 ± 0.7117 ng/ml, respectively, $p = 0.0011$; Fig. 5A). Similarly, the concentration of vascular endothelial growth factor (VEGF), the key regulator of tumor angiogenesis, was also significantly elevated in patients with melanoma (vs. controls, 0.0689 ± 0.0086 ng/ml vs. 0.0454 ± 0.0128 , respectively, $p < 0.0001$; Fig. 5B).

Furthermore, in order to study the clinical relevance of expression level of apelin gene in patients with melanoma, we performed comparative statistical analyses using several publicly available datasets (Supp Fig. 3A,B). According to the Gene Expression Profiling Interactive Analysis 2 (GEPIA2) database, patients with high apelin expression levels ($n = 229$) have significantly impaired survival outcomes than those with low apelin-expressing

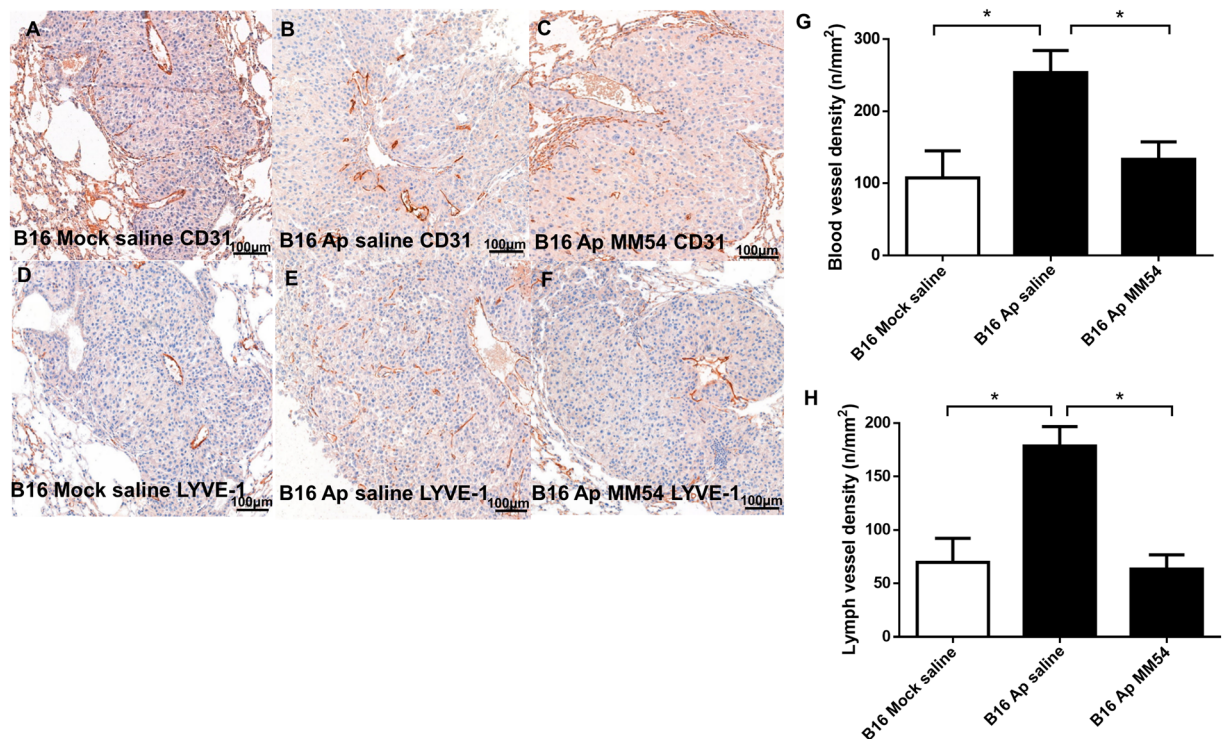


Figure 3. Apelin has (lymph)angiogenic effect in mouse pulmonary metastases, which can be attenuated by MM54. Paraffin-embedded sections of lung metastases of apelin-overexpressing B16 Ap and B16 Mock cells were stained for the blood endothelial cell marker CD31 (A–C) and the lymphatic endothelial cell marker LYVE-1 (D–F). (G,H) Apelin overexpression significantly increased both the blood vessel (G) and lymph vessel (H) densities. This effect was attenuated by APJ receptor antagonist MM54 (G,H). * $p < 0.05$.

tumors ($n = 229$; $p = 0.038$) in the case of patients with skin cutaneous melanoma (Supp Fig. 3A)⁵⁴. PrognScan database analyzed a patient cohort of 38 samples based on the HG-U133_Plus_2 microarray data, and also suggested that high expression levels of apelin gene are potential negative prognosticators in patients with melanoma (the corrected p value = 0.0405; Supp Fig. 3B)⁵⁵. In addition, Tumor Immune Estimation Resource 2.0 (TIMER 2.0) and the Human Protein Atlas also showed a tendency towards poor prognosis in patients with high apelin levels, when analyzing the associations between the expression levels of apelin gene and survival outcomes in TCGA: TIMER 2.0 analyzed 471 patients with skin cutaneous melanoma ($p = 0.065$); the Human Protein Atlas studied 102 patients ($p = 0.047$; data not shown)^{56,57}.

Discussion

Malignant melanoma is an aggressive tumor with high metastatic potential^{1,3}. It can disseminate to multiple organs with a generally poor prognosis, if not treated with the new drugs like BRAF-, MEK inhibitors and immunomodulators^{2–4,6,7}.

Apelin, a ligand of the G-protein-coupled APJ receptor was identified in 1998 by Tatemoto and coworkers¹⁰. Since then, several studies demonstrated that apelin is a potent activator of tumor neoangiogenesis^{16,19,20,22,58}. Additionally, apelin was reported to promote lymphangiogenesis and lymph node metastasis²⁴.

On the basis of a human cancer profiling array, Sorli et al. reported that the apelin gene is upregulated with a very high frequency in skin cancers²⁰, but there is lack of knowledge on the role of apelin molecule in cutaneous melanoma. In the current study, we investigated the role of apelin in lung metastases of this malignancy and validated apelin signaling as a new potential therapeutic target.

As a first step, we performed sulforhodamine B (SRB) assay with the control and apelin-overexpressing B16 and A375 cells and found that apelin had no impact on the proliferation of melanoma cell lines in two-dimensional cell cultures. Feng et al. showed similar results in gastric cancer, while apelin significantly enhanced the proliferation rate of oral cell carcinoma²⁷ and breast cancer cells via the extracellular signal-regulated kinase (Erk) signaling pathway⁵⁹. We found that apelin overexpression induced a more invasive phenotype in 3D collagen invasion assay and promoted migration on plastic and on collagen as well. In the abovementioned studies, apelin treatment significantly increased tumor cell migration and invasion, and, moreover, it also induced the expression of several invasion and metastasis-related cytokines, e.g. matrix metalloproteinase-1 (MMP-1), matrix metalloproteinase-9 (MMP-9), interleukin-2 (IL-2) and interleukin-6 (IL-6)^{26,59,60}.

In a metastatic mice model, where the tumor cells were injected intravenously, we found that apelin overexpression significantly increased both the number and size of lung metastases. Histological analysis of the tumors revealed that blood and lymph vessel densities were significantly higher in B16 Ap tumors, resulting in increased

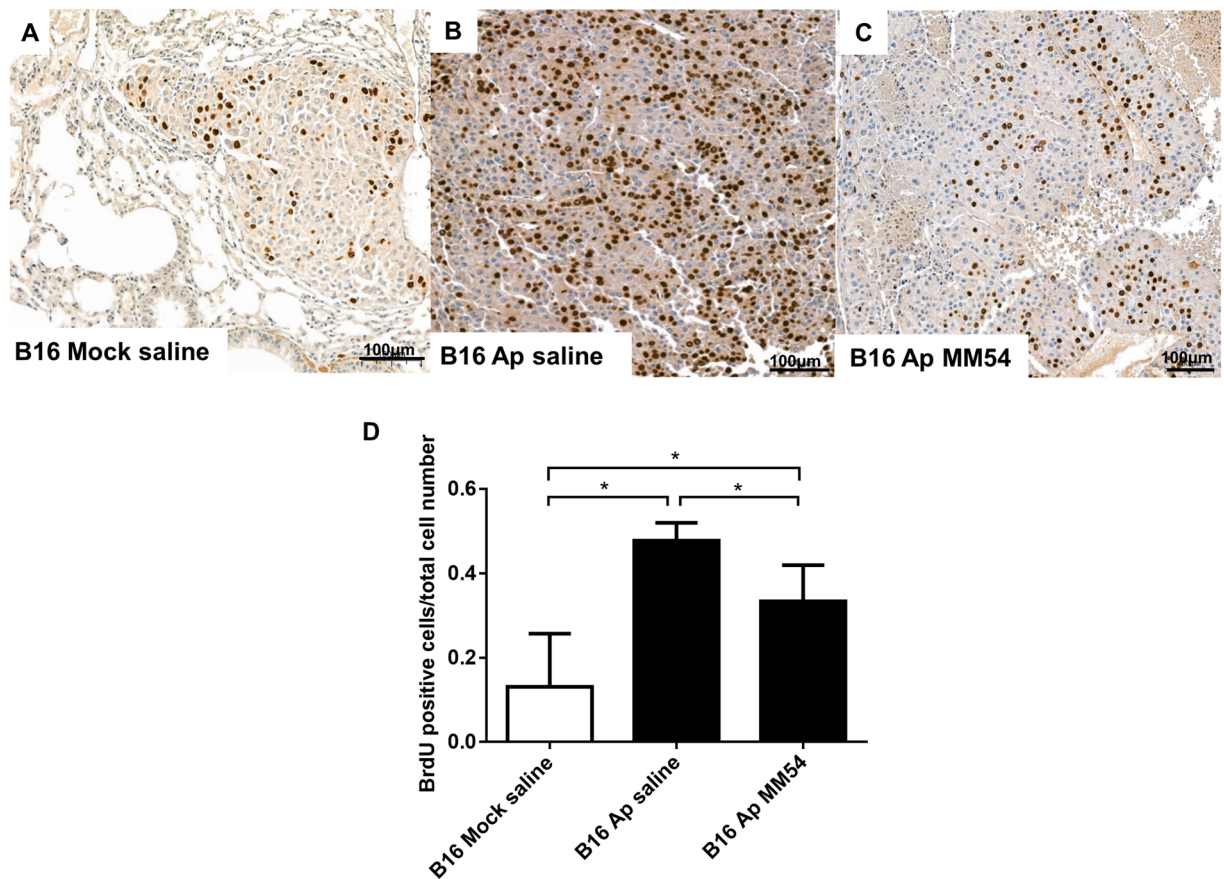


Figure 4. Apelin overexpression increases tumor cell proliferation in lung metastases, which can be attenuated by MM54. (A–C) Representative images of lung metastases from a mouse injected with B16 Ap and B16 Mock cells. BrdU-positive cells were visualized with 3-amino-9-ethylcarbazole (AEC) peroxidase substrate solution. (D) Apelin overexpression significantly increased the number of BrdU-positive tumor cells in B16 lung metastases, and this effect was significantly attenuated by APJ receptor antagonist MM54. * $p < 0.05$.

tumor cell proliferation. We reported earlier that apelin enhances the growth of subcutaneously inoculated B16 tumors and promotes lymphangiogenesis. We hypothesized that tumour growth might be enhanced by a stimulatory effect of apelin on lymph vessel formation²⁴. In a breast cancer model, the degree of tumor lymphangiogenesis was found to be correlated with lymph node metastases⁶¹. Furthermore, apelin induced tumor growth in murine models of mammary and hepatocellular carcinoma by promoting angiogenesis^{23,34}. Overexpression of APJ, the receptor of apelin increased peritoneal metastasis in ovarian cancer³⁹.

In our study, MM54, a competitive APJ antagonist, inhibited tumor (lymph)angiogenesis and tumor cell proliferation and thus attenuated apelin-induced growth of melanoma lung metastasis. MM54 previously reduced glioblastoma growth in an ectopic xenograft tumor model and prolonged the survival of tumor-bearing mice⁶². In line with the abovementioned study, we also showed that the decreased tumor growth is associated with a reduction of tumor cell proliferation and vascularization.

Having demonstrated that apelin promotes metastatic growth in preclinical models of murine and human melanoma, we next investigated the clinical relevance of this observation. Circulating levels of apelin were measured in 40 blood samples of melanoma patients. Apelin levels were significantly elevated in patients' blood compared to control individuals. Similar findings were reported in colorectal cancer, where apelin and its receptor had higher expression in tumor tissue and serum samples of patients³⁸. Importantly, in this study from Podgorska et al. high circulating apelin levels were associated with the presence of lymph node and distant metastasis. Blood apelin levels were also reported to be elevated in breast³⁷, head and neck³⁶ and gastroesophageal cancer²⁵. In contrast, plasma apelin levels in lung cancer patients were reported significantly lower than in healthy controls²⁹. In gastric cancer, tumor apelin levels were elevated, but, interestingly, this was not reflected by higher circulating apelin levels²⁶.

We also report significantly elevated VEGF levels in melanoma patients. Uribealago et al. recently showed that apelin ablation enhances effectiveness of anti-angiogenic treatment in preclinical models of mammary and lung cancer and, furthermore, that blocking apelin prevents sunitinib-induced metastases. Moreover, high apelin levels correlated with poor prognosis of renal cell carcinoma patients on sunitinib therapy²³. When these authors investigated the expression of apelin and VEGF, the key regulator of angiogenesis, they found that patients with both low apelin and low VEGF serum levels had the best prognosis, while patients with high levels of these proteins

Characteristics	Patients with melanoma (n = 40)		Healthy controls (n = 21)	
	Numbers	%	Numbers	%
Gender				
Male	19	47.5	11	52
Female	21	52.5	10	48
Age (years)				
< 60	13	32.5	18	86
≥ 60	26	65	3	14
NA	1	2.5	0	0
Co-morbidities				
Arterial hypertension	14	35	0	0
Cardiovascular diseases	13	32.5	0	0
Diabetes	5	12.5	0	0
Inflammatory diseases	3	7.5	0	0
Asthma	1	2.5	0	0
Renal disease	1	2.5	0	0
None	9	22.5	21	100
Breslow depth (mm)				
< 0.75 mm	2	5		
0.76–3.99 mm	25	62.5		
> 4 mm	10	25		
NA	3	7.5		
Histological subtype				
SMM	14	35		
NMM	8	20		
ALM	2	5		
NA	16	40		
Treatment				
Immunotherapy	7	17.5		
Radiotherapy	5	12.5		
Immuno + Radiotherapy	5	12.5		
BRAF + MEK1.2 inhibitors	3	7.5		
Other	5	12.5		
None	13	32.5		
NA	2	5		

Table 1. Clinical characteristics of patients with melanoma and healthy controls. 40 patients with melanoma and 21 healthy individuals were included in the study. *SMM* superficial malignant melanoma, *NMM* nodular malignant melanoma, *ALM* acral lentiginous melanoma, *NA* not available.

had shortest median progression-free survival²³, suggesting that both apelin and VEGF interact in determining clinical outcome. We also analyzed publicly available databases to explore associations between apelin gene expression and clinical outcome in patients with melanoma. These results suggested that the expression level of apelin gene is a potential prognostic marker in patients with skin cutaneous melanoma^{54–57}.

In conclusion, our results suggest that apelin signaling plays an important role in the pulmonary metastasis formation of cutaneous melanoma. Therefore, novel drugs targeting apelin signaling might offer benefits to patients with this devastating disease and could lead to the improvement of the outcome of patients with this malignancy.

Materials and methods

Cell lines. The B16 mouse melanoma cells stably transfected with murine apelin (B16 Ap) or with the empty plasmid vector (B16 Mock) have been previously described in ref.⁶³. The A375 human melanoma cell line was obtained from the American Type Culture Collection (Manassas, VA). All cell lines were maintained in Dulbecco's modified Eagle's medium (DMEM; Sigma Aldrich Corp., St. Louis, MO, USA) supplemented with 10% fetal bovine serum (FBS; Sigma Aldrich Corp.) and 1% penicillin/streptomycin (Sigma Aldrich Corp.) at 37 °C in a humidified incubator with 5% CO₂.

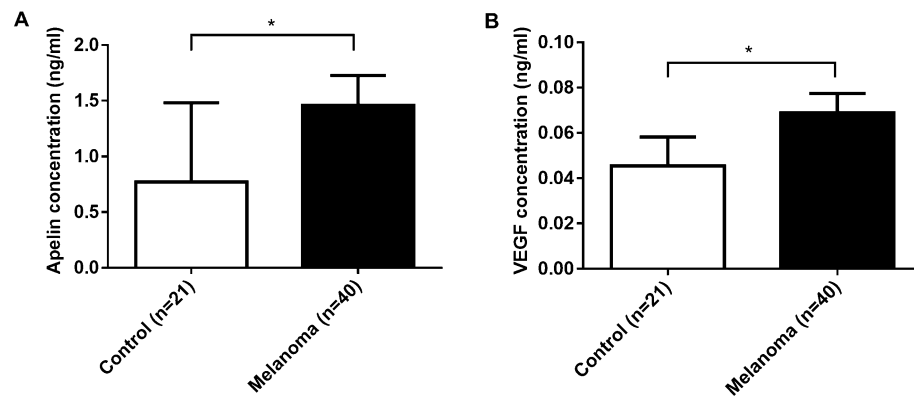


Figure 5. Apelin and VEGF plasma levels are elevated in patients with melanoma vs. healthy group. **(A)** Plasma apelin levels were significantly elevated in patients with melanoma ($n = 40$) compared to those in the healthy group ($n = 21$) (1.4590 ± 0.2676 ng/ml vs. 0.7704 ± 0.7117 ng/ml, respectively, $p = 0.0011$). **(B)** Plasma VEGF levels were significantly higher in patients with melanoma (vs. healthy controls), (0.0689 ± 0.0086 ng/ml vs. 0.0454 ± 0.0128 , respectively, $p < 0.0001$). * $p < 0.05$.

Three-dimensional spheroid invasion assay. For invasion assay, spheroids formed by the B16 and A375 cells in 2% agarose gel (Sigma Aldrich Co.) using MicroTissues 3D Petri Dish (Sigma Aldrich Co.) were put in 96-well plate with 10% FBS-containing DMEM medium and collagen I (Corning, Corning, NY, USA), $10 \times$ Dulbecco's Phosphate Buffered Saline (Sigma Aldrich Co.) and 1 M NaOH containing gel. After solidifying the gel, it was covered with medium. After 48 h, the spheroids were photographed in each well. The extent of invasion was estimated from perimeter/area ratio of spheroids using ImageJ software.

Videomicroscopic measurements of 2D cell migration and 3D invasion. For 2D migration assay, B16 Mock, B16 Ap, A375 Mock and A375 Ap cells were seeded at densities of 90/30/10 cells/mm² into 6 mm diameter polylactic acid mini-wells, 3D printed into 35 mm culture dishes (Greiner Bio-One, North Carolina, USA)⁶⁴. For videomicroscopic measurements of 3D invasion assay, single cell suspensions of B16 and A375 cells were mixed in 30 μ l of 1.7 mg/ml Collagen-I gel (Corning) at a final cell density of 30 000 cells/ml.

Time-lapse recordings were performed on a computer-controlled Leica DM IRB inverted microscope equipped with a Marzhauser SCAN-IM powered stage and a $10 \times$ N-PLAN objective with 0.25 numerical aperture and 5.8 mm working distance. The microscope was coupled to an Olympus DP70 colour CCD camera. Cell cultures were kept at 37 °C in humidified 5% CO₂ atmosphere in a stage-top mini incubator during imaging. Phase contrast images of cells were collected every 10 min from 9 microscopic fields for 3 days.

Recorded phase-contrast images were analyzed by particle image velocimetry (PIV) method^{65,66}. To detect cell occupied area a global threshold was applied to the local standard deviation of intensity on each image^{67,68}. To obtain cell speeds, PIV displacements restricted to cell-occupied areas were normalized by the time lag between the two frames (10 min) compared with the PIV method. In each experiment, data from 9 microscopic fields were averaged, and experiments were replicated twice.

In vivo studies of tumor growth. Pulmonary metastasis formation of the apelin-transfected B16 melanoma cells was compared with that of control vector expressing cells in 9-week-old C57Bl/6 mice. According to the institutional animal welfare guidelines, all mice were maintained on a daily 12-h light/12-h dark cycle and were housed under pathogen-free conditions in microisolator cages with laboratory chow and water ad libitum. Apelin-overexpressing and control melanoma cells were grown to 80% confluence, harvested by trypsinization and washed twice with phosphate buffered saline (PBS). Lung metastases were established by injecting 2×10^5 B16 Ap or B16 Mock cells intravenously into the tail vein of mice. To study the effect of MM54 (Tocris Biotechnique Corp., Minneapolis, MN, USA), the APJ receptor antagonist on the growth of lung metastases, mice injected with B16 Ap cells were treated twice per week with MM54 (2 mg/kg) or, in case of the mice injected with B16 Ap or B16 Mock cells, with saline by intraperitoneal injection⁶². Lungs were harvested 3 weeks after tumor cell inoculation. For labelling proliferating cells, 240 mg/kg 5-bromo-2'-deoxyuridine (BrdU; Sigma Aldrich Corp.) in saline was injected intraperitoneally into mice 1.5 h before lethal anesthesia. Lungs were fixed in BrdU fixing solution after removal. The number of lung metastases was counted by stereomicroscope and their length and width were measured by ocular micrometer. The tumor volume was calculated by use of the modified ellipsoid formula $1/2(\text{Length} \times \text{Width}^2)$ ⁶⁹. The animals used in this study were cared according to the "Guiding Principles for the Care and Use of Animals" based upon the Helsinki declaration. The animal-model experiments were carried out in compliance with the ARRIVE guidelines and approved by the Ethics Committee of the Department of Food Chain Safety, Animal Health, Plant and Soil Protection, Pest County Government Office (license number: PEI/001/2574-6/2015).

5-bromo-2'-deoxyuridine (BrdU) incorporation and BrdU immunohistochemical stainings on lung metastases. For labelling proliferating cells, 240 mg/kg 5-bromo-2'-deoxyuridine (Sigma Aldrich Corp.) was injected intraperitoneally into mice 1.5 h before lethal anesthesia. Lungs were fixed in BrdU fixing solution after removal. Five-micrometer paraffin sections were dewaxed and rehydrated. The peroxidase was quenched with methanol and H₂O₂ for 30 min. The slides were then incubated with HCl for 15 min, and blocked with milk powder for 30 min. BrdU immunostaining was performed using a mouse monoclonal anti-BrdU antibody (Becton Dickinson). The binding of BrdU was visualized by Dako Real Detection System (Agilent, Santa Clara, CA, USA) following the instructions of the manufacturer. The slides were scanned by PANNORAMIC 1000 slide digitalization system (3DHitech, Budapest, Hungary). One thousand nuclei per lung were counted on digital photographs using QuantCenter software (3DHitech, Budapest, Hungary).

Immunohistochemical stainings of blood and lymph vessels in lung metastases of mice. Immunohistochemical (IHC) stainings were performed on fixed samples embedded in paraffin. Five-micrometer paraffin sections were dewaxed and rehydrated. The peroxidase was quenched with methanol and 3% H₂O₂ for 15 min. For stainings of blood and lymph vessels, antigen retrieval was performed in 0.1 M citrate buffer (pH = 6; Agilent) in hot water bath at 98 °C for 45 min. The slides were then incubated with 3% bovine serum albumin (BSA; Sigma Aldrich Corp.) in phosphate buffered saline (Sigma Aldrich Corp.) for blocking non-specific protein binding. Slides were then incubated with antibodies to rat anti-mouse CD31 (Dianova, Hamburg, Germany) and rabbit anti-mouse lymphatic vessel endothelial receptor 1 (LYVE-1; ReliaTech, Wolfenbüttel, Germany). Rabbit anti-rat IgG (Novus Biologicals, Colorado, CO, USA) was used as secondary antibody in the case of CD31 primary antibody. The antibodies were detected with Dako Real Detection System, Peroxidase/AEC, Rabbit/Mouse (Agilent). Finally, counterstaining was performed using Mayer's modified hematoxylin (Bio-Optica, Milano, Italy). CD31- or LYVE-1-stained vessels were counted at three randomly selected fields per lung on digital photographs using QuantCenter software (3DHitech) to calculate blood or lymph vessel densities, respectively.

Patients material. Plasma samples of patients with melanoma (n = 40) were collected between 2011 and 2017 at the Department of Surgery, Lund University Hospital. Additional plasma samples from healthy individuals (n = 21) were also analyzed. The study was conducted in accordance with the current National Comprehensive Cancer Network guidelines, based on the ethical standards prescribed by the Helsinki Declaration of the World Medical Association. All patients and controls had given informed consent, and the sample collection was approved by the Regional Ethical Review Board in Lund (approval numbers: DNR 2013/101 and DNR 2013/480).

Collection of blood samples. Blood samples were aliquoted and stored in the BioMEL Biobank Lund University. Vacutainer Ethylenediaminetetraacetic acid (EDTA) Blood Collection tubes (Becton Dickinson, Franklin Lakes, NJ, USA) were centrifuged at 2000 g for 10 min at room temperature. The automatic aliquoting of samples were performed by a robot (Hamilton robot MicroLab Starlet, Hamilton, Bonaduz AG, Switzerland). The 70 µl aliquot vials were sealed with aluminum foil and stored in 384-well plates at -80 °C in a fully automated biobank storage unit (LICONIC freezer STT1k5 ULT, Liconic AG, Mauren, Liechtenstein)^{70,71}.

Enzyme-linked immunosorbent assays (ELISAs). Apelin-36 and VEGF ELISA kits were purchased from Phoenix Pharmaceutical (EKE-057-15, Burlingame, CA, USA) and R&D Systems (DVE00, Minneapolis, MN, USA), respectively. All plasma samples and kit components were equilibrated to room temperature before assay. Sample preparation and detection procedures were performed in accordance with the manufacturer's manual.

Statistical analysis. In case of two groups, the continuous variables were compared with Student's *t* test if the sample distribution was normal or with Mann-Whitney U test if the sample distribution was asymmetric. Tukey's multiple comparison test were used for more than two groups. Differences were determined to be significant if *p* < 0.05. All statistical analyses were done using GraphPad Prism 6.0 (GraphPad Software, Inc., La Jolla, CA, USA) and IBM SPSS Statistics 23 software (IBM Corp., Armonk, NY, USA).

Ethics approval and consent to participate. The study was conducted in accordance with the current National Comprehensive Cancer Network guidelines, based on the ethical standards prescribed by the Helsinki Declaration of the World Medical Association. All patients and controls had given informed consent, and the sample collection was approved by the Regional Ethical Review Board in Lund (Approval Numbers: DNR 2013/101 and DNR 2013/480).

The animals used in this study were cared according to the "Guiding Principles for the Care and Use of Animals" based upon the Helsinki declaration. The animal-model experiments were carried out in compliance with the ARRIVE guidelines and approved by the Ethics Committee of the Department of Food Chain Safety, Animal Health, Plant and Soil Protection, Pest County Government Office (License Number: PEI/001/2574-6/2015).

Data availability

The datasets used and analyzed during the current study are available from the corresponding authors on reasonable request.

Received: 28 September 2020; Accepted: 24 February 2021

Published online: 11 March 2021

References

- Emmett, M. S., Dewing, D. & Pritchard-Jones, R. O. Angiogenesis and melanoma—from basic science to clinical trials. *Am. J. Cancer Res.* **1**, 852–868 (2011).
- Finn, L., Markovic, S. N. & Joseph, R. W. Therapy for metastatic melanoma: the past, present, and future. *BMC Med.* **10**, 23. <https://doi.org/10.1186/1741-7015-10-23> (2012).
- Grossman, D. & Altieri, D. C. Drug resistance in melanoma: mechanisms, apoptosis, and new potential therapeutic targets. *Cancer Metastasis Rev.* **20**, 3–11 (2001).
- Chapman, P. B. *et al.* Improved survival with vemurafenib in melanoma with BRAF V600E mutation. *N. Engl. J. Med.* **364**, 2507–2516. <https://doi.org/10.1056/NEJMoa1103782> (2011).
- Robert, C. *et al.* Nivolumab in previously untreated melanoma without BRAF mutation. *N. Engl. J. Med.* **372**, 320–330. <https://doi.org/10.1056/NEJMoa1412082> (2015).
- Robert, C. *et al.* Five-year outcomes with dabrafenib plus trametinib in metastatic melanoma. *N. Engl. J. Med.* **381**, 626–636. <https://doi.org/10.1056/NEJMoa1904059> (2019).
- Robert, C. *et al.* Improved overall survival in melanoma with combined dabrafenib and trametinib. *N. Engl. J. Med.* **372**, 30–39. <https://doi.org/10.1056/NEJMoa1412690> (2015).
- Robert, C. *et al.* Pembrolizumab versus Ipilimumab in Advanced Melanoma. *N. Engl. J. Med.* **372**, 2521–2532. <https://doi.org/10.1056/NEJMoa1503093> (2015).
- Robert, C. *et al.* Ipilimumab plus dacarbazine for previously untreated metastatic melanoma. *N. Engl. J. Med.* **364**, 2517–2526. <https://doi.org/10.1056/NEJMoa1104621> (2011).
- Tatemoto, K. *et al.* Isolation and characterization of a novel endogenous peptide ligand for the human APJ receptor. *Biochem. Biophys. Res. Commun.* **251**, 471–476. <https://doi.org/10.1006/bbrc.1998.9489> (1998).
- Kleinz, M. J. & Davenport, A. P. Emerging roles of apelin in biology and medicine. *Pharmacol. Ther.* **107**, 198–211. <https://doi.org/10.1016/j.pharmthera.2005.04.001> (2005).
- Beltowski, J. Apelin and visfatin: unique “beneficial” adipokines upregulated in obesity?. *Med. Sci. Monit.* **12**, 112–119 (2006).
- Castan-Laurell, I., Masri, B. & Valet, P. The apelin/APJ system as a therapeutic target in metabolic diseases. *Expert Opin. Ther. Targets* **23**, 215–225. <https://doi.org/10.1080/14728222.2019.1561871> (2019).
- Chapman, N. A., Dupre, D. J. & Rainey, J. K. The apelin receptor: physiology, pathology, cell signalling, and ligand modulation of a peptide-activated class A GPCR. *Biochem. Cell Biol.* **92**, 431–440. <https://doi.org/10.1139/bcb-2014-0072> (2014).
- Eyries, M. *et al.* Hypoxia-induced apelin expression regulates endothelial cell proliferation and regenerative angiogenesis. *Circ. Res.* **103**, 432–440. <https://doi.org/10.1161/CIRCRESAHA.108.179333> (2008).
- Kasai, A. *et al.* Apelin is a novel angiogenic factor in retinal endothelial cells. *Biochem. Biophys. Res. Commun.* **325**, 395–400. <https://doi.org/10.1016/j.bbrc.2004.10.042> (2004).
- Cox, C. M., D’Agostino, S. L., Miller, M. K., Heimark, R. L. & Krieg, P. A. Apelin, the ligand for the endothelial G-protein-coupled receptor, APJ, is a potent angiogenic factor required for normal vascular development of the frog embryo. *Dev. Biol.* **296**, 177–189. <https://doi.org/10.1016/j.ydbio.2006.04.452> (2006).
- Kleinz, M. J. & Davenport, A. P. Immunocytochemical localization of the endogenous vasoactive peptide apelin to human vascular and endocardial endothelial cells. *Regul. Pept.* **118**, 119–125. <https://doi.org/10.1016/j.regpep.2003.11.002> (2004).
- Kalin, R. E. *et al.* Paracrine and autocrine mechanisms of apelin signaling govern embryonic and tumor angiogenesis. *Dev. Biol.* **305**, 599–614. <https://doi.org/10.1016/j.ydbio.2007.03.004> (2007).
- Sorli, S. C., Le Gonidec, S., Knibiehler, B. & Audigier, Y. Apelin is a potent activator of tumour neoangiogenesis. *Oncogene* **26**, 7692–7699. <https://doi.org/10.1038/sj.onc.1210573> (2007).
- Berta, J. *et al.* Apelin expression in human non-small cell lung cancer: role in angiogenesis and prognosis. *J. Thorac. Oncol.* **5**, 1120–1129. <https://doi.org/10.1097/JTO.0b013e3181e2c1ff> (2010).
- Kidoya, H. *et al.* The apelin/APJ system induces maturation of the tumor vasculature and improves the efficiency of immune therapy. *Oncogene* **31**, 3254–3264. <https://doi.org/10.1038/nc.2011.489> (2012).
- Uribealago, I. *et al.* Apelin inhibition prevents resistance and metastasis associated with anti-angiogenic therapy. *EMBO Mol. Med.* **11**, e9266. <https://doi.org/10.15252/emmm.201809266> (2019).
- Berta, J. *et al.* Apelin promotes lymphangiogenesis and lymph node metastasis. *Oncotarget* **5**, 4426–4437. <https://doi.org/10.18632/oncotarget.2032> (2014).
- Diakowska, D., Markocka-Maczka, K., Szelachowski, P. & Grabowski, K. Serum levels of resistin, adiponectin, and apelin in gastroesophageal cancer patients. *Dis. Markers* **2014**, 619649. <https://doi.org/10.1155/2014/619649> (2014).
- Feng, M., Yao, G., Yu, H., Qing, Y. & Wang, K. Tumor apelin, not serum apelin, is associated with the clinical features and prognosis of gastric cancer. *BMC Cancer* **16**, 794. <https://doi.org/10.1186/s12885-016-2815-y> (2016).
- Heo, K. *et al.* Hypoxia-induced up-regulation of apelin is associated with a poor prognosis in oral squamous cell carcinoma patients. *Oral Oncol.* **48**, 500–506. <https://doi.org/10.1016/j.oraloncology.2011.12.015> (2012).
- Lacquanti, A. *et al.* Apelin beyond kidney failure and hyponatremia: a useful biomarker for cancer disease progression evaluation. *Clin. Exp. Med.* **15**, 97–105. <https://doi.org/10.1007/s10238-014-0272-y> (2015).
- Ni, Y. *et al.* Apelin is a novel circulating biomarker for the diagnosis of lung cancer. *Int. J. Clin. Exp. Pathol.* **10**(5), 5559–5565 (2017).
- Wan, Y. *et al.* Dysregulated microRNA-224/apelin axis associated with aggressive progression and poor prognosis in patients with prostate cancer. *Hum. Pathol.* **46**, 295–303. <https://doi.org/10.1016/j.humpath.2014.10.027> (2015).
- Yang, Y., Lv, S. Y., Ye, W. & Zhang, L. Apelin/APJ system and cancer. *Clin. Chim. Acta Int. J. Clin. Chem.* **457**, 112–116. <https://doi.org/10.1016/j.cca.2016.04.001> (2016).
- Yang, L., Li, Y. L., Li, X. Q. & Zhang, Z. High Apelin level indicates a poor prognostic factor in muscle-invasive bladder cancer. *Dis. Markers* **2019**, 4586405. <https://doi.org/10.1155/2019/4586405> (2019).
- Chen, H. *et al.* APLN promotes hepatocellular carcinoma through activating PI3K/Akt pathway and is a druggable target. *Theranostics* **9**, 5246–5260. <https://doi.org/10.7150/thno.34713> (2019).
- Muto, J. *et al.* The apelin-APJ system induces tumor arteriogenesis in hepatocellular carcinoma. *Anticancer Res.* **34**, 5313–5320 (2014).
- Vachher, M., Arora, K., Burman, A. & Kumar, B. NAMPT, GRN, and SERPINE1 signature as predictor of disease progression and survival in gliomas. *J. Cell Biochem.* <https://doi.org/10.1002/jcb.29560> (2019).
- Aktan, M. & Ozmen, H. K. A preliminary study of serum apelin levels in patients with head and neck cancer. *Eurasian J. Med.* **51**, 57–59. <https://doi.org/10.5152/eurasianjmed.2018.18411> (2019).
- Salman, T. *et al.* Serum apelin levels and body composition changes in breast cancer patients treated with an aromatase inhibitor. *JBUNON* **21**, 1419–1424 (2016).
- Podgorska, M., Diakowska, D., Pietraszek-Gremplewicz, K., Nienartowicz, M. & Nowak, D. Evaluation of apelin and apelin receptor level in the primary tumor and serum of colorectal cancer patients. *J. Clin. Med.* <https://doi.org/10.3390/jcm8101513> (2019).

39. Neelakantan, D. *et al.* Multifunctional APJ pathway promotes ovarian cancer progression and metastasis. *Mol. Cancer Res.* **17**, 1378–1390. <https://doi.org/10.1158/1541-7786.MCR-18-0989> (2019).
40. Leo, F. *et al.* Lung metastases from melanoma: when is surgical treatment warranted?. *Br. J. Cancer* **83**, 569–572. <https://doi.org/10.1054/bjoc.2000.1335> (2000).
41. Velu, P. P., Cao, C. & Yan, T. D. Current surgical management of melanoma metastases to the lung. *J. Thorac. Dis.* **5**(Suppl 3), S274–276. <https://doi.org/10.3978/j.issn.2072-1439.2013.08.42> (2013).
42. Tolkach, Y. *et al.* Apelin and apelin receptor expression in renal cell carcinoma. *Br. J. Cancer* **120**, 633–639. <https://doi.org/10.1038/s41416-019-0396-7> (2019).
43. Patel, S. J. *et al.* Identification of essential genes for cancer immunotherapy. *Nature* **548**, 537–542. <https://doi.org/10.1038/nature23477> (2017).
44. Samura, M. *et al.* Combinatorial treatment with apelin-13 enhances the therapeutic efficacy of a preconditioned cell-based therapy for peripheral ischemia. *Sci. Rep.* **6**, 19379. <https://doi.org/10.1038/srep19379> (2016).
45. Qin, D., Zheng, X. X. & Jiang, Y. R. Apelin-13 induces proliferation, migration, and collagen I mRNA expression in human RPE cells via PI3K/Akt and MEK/Erk signaling pathways. *Mol. Vis.* **19**, 2227–2236 (2013).
46. De Wever, O. *et al.* Modeling and quantification of cancer cell invasion through collagen type I matrices. *Int. J. Dev. Biol.* **54**, 887–896. <https://doi.org/10.1387/ijdb.092948ow> (2010).
47. Vinci, M., Box, C. & Eccles, S. A. Three-dimensional (3D) tumor spheroid invasion assay. *J. Vis. Exp.: JoVE* <https://doi.org/10.3791/52686> (2015).
48. Yang, L. *et al.* ERK1/2 mediates lung adenocarcinoma cell proliferation and autophagy induced by apelin-13. *Acta Biochim. Biophys. Sin.* **46**, 100–111. <https://doi.org/10.1093/abbs/gmt140> (2014).
49. Jin, G. *et al.* Association of brain natriuretic peptide gene polymorphisms with chronic obstructive pulmonary disease complicated with pulmonary hypertension and its mechanism. *Biosci. Rep.* <https://doi.org/10.1042/BSR20180905> (2018).
50. Lv, D., Li, H. & Chen, L. Apelin and APJ, a novel critical factor and therapeutic target for atherosclerosis. *Acta Biochim. Biophys. Sin.* **45**, 527–533. <https://doi.org/10.1093/abbs/gmt040> (2013).
51. Machura, E. *et al.* Serum apelin-12 level is elevated in schoolchildren with atopic asthma. *Respir. Med.* **107**, 196–201. <https://doi.org/10.1016/j.rmed.2012.10.026> (2013).
52. Wysocka, M. B., Pietraszek-Gremplewicz, K. & Nowak, D. The role of apelin in cardiovascular diseases, obesity and cancer. *Front. Physiol.* **9**, 557. <https://doi.org/10.3389/fphys.2018.00557> (2018).
53. Zhong, J. C. *et al.* Targeting the apelin pathway as a novel therapeutic approach for cardiovascular diseases. *Biochim Biophys. Acta Mol. Basis Dis.* **1942–1950**, 2017. <https://doi.org/10.1016/j.bbadis.2016.11.007> (1863).
54. Tang, Z., Kang, B., Li, C., Chen, T. & Zhang, Z. GEPIA2: an enhanced web server for large-scale expression profiling and interactive analysis. *Nucleic Acids Res.* **47**, W556–W560. <https://doi.org/10.1093/nar/gkz430> (2019).
55. Mizuno, H., Kitada, K., Nakai, K. & Sarai, A. Prognoscan: a new database for meta-analysis of the prognostic value of genes. *BMC Med. Genomics* **2**, 18. <https://doi.org/10.1186/1755-8794-2-18> (2009).
56. Li, T. *et al.* TIMER2.0 for analysis of tumor-infiltrating immune cells. *Nucleic Acids Res.* **48**, W509–W514. <https://doi.org/10.1093/nar/gkaa407> (2020).
57. Uhlen, M. *et al.* A pathology atlas of the human cancer transcriptome. *Science* <https://doi.org/10.1126/science.aan2507> (2017).
58. Kidoya, H. *et al.* Spatial and temporal role of the apelin/APJ system in the caliber size regulation of blood vessels during angiogenesis. *EMBO J.* **27**, 522–534. <https://doi.org/10.1038/sj.emboj.7601982> (2008).
59. Peng, X. *et al.* Apelin-13 induces MCF-7 cell proliferation and invasion via phosphorylation of ERK1/2. *Int. J. Mol. Med.* **36**, 733–738. <https://doi.org/10.3892/ijmm.2015.2265> (2015).
60. Podgorska, M., Pietraszek-Gremplewicz, K. & Nowak, D. Apelin effects migration and invasion abilities of colon cancer cells. *Cells* <https://doi.org/10.3390/cells7080113> (2018).
61. Mattila, M. M. *et al.* VEGF-C induced lymphangiogenesis is associated with lymph node metastasis in orthotopic MCF-7 tumors. *Int. J. Cancer* **98**, 946–951. <https://doi.org/10.1002/ijc.10283> (2002).
62. Harford-Wright, E. *et al.* Pharmacological targeting of apelin impairs glioblastoma growth. *Brain* **140**, 2939–2954. <https://doi.org/10.1093/brain/awx253> (2017).
63. Sorli, S. C., van den Berghe, L., Masri, B., Knibiehler, B. & Audigier, Y. Therapeutic potential of interfering with apelin signalling. *Drug Discov. Today* **11**, 1100–1106. <https://doi.org/10.1016/j.drudis.2006.10.011> (2006).
64. Gulyas, M., Csiszer, M., Mehes, E. & Czirok, A. Software tools for cell culture-related 3D printed structures. *PLoS ONE* **13**, e0203203. <https://doi.org/10.1371/journal.pone.0203203> (2018).
65. Zamir, E. A., Czirok, A., Rongish, B. J. & Little, C. D. A digital image-based method for computational tissue fate mapping during early avian morphogenesis. *Ann. Biomed. Eng.* **33**, 854–865 (2005).
66. Czirok, A. *et al.* Optical-flow based non-invasive analysis of cardiomyocyte contractility. *Sci. Rep.* **7**, 10404. <https://doi.org/10.1038/s41598-017-10094-7> (2017).
67. Wu, K., Gauthier, D. & Levine, M. D. Live cell image segmentation. *IEEE Trans. Biomed. Eng.* **42**, 1–12 (1995).
68. Neufeld, Z. *et al.* The role of Allee effect in modelling post resection recurrence of glioblastoma. *PLoS Comput. Biol.* **13**, e1005818. <https://doi.org/10.1371/journal.pcbi.1005818> (2017).
69. Jensen, M. M., Jorgensen, J. T., Binderup, T. & Kjaer, A. Tumor volume in subcutaneous mouse xenografts measured by microCT is more accurate and reproducible than determined by 18F-FDG-microPET or external caliper. *BMC Med. Imaging* **8**, 16. <https://doi.org/10.1186/1471-2342-8-16> (2008).
70. Truedsson, M. *et al.* Biomarkers of early chronic obstructive pulmonary disease (COPD) in smokers and former smokers. Protocol of a longitudinal study. *Clin. Transl. Med.* <https://doi.org/10.1186/s40169-016-0086-5> (2016).
71. Eriksson, J. *et al.* Merging clinical chemistry biomarker data with a COPD database—building a clinical infrastructure for proteomic studies. *Proteome Sci.* **15**, 8. <https://doi.org/10.1186/s12953-017-0116-2> (2016).

Acknowledgements

We would like to thank Dóra Lakatos, the member of the Department of Biological Physics, Eötvös University for helping to evaluate the videomicroscopic measurements. We also specially thank Zsófia Szabó-Zsibai for scanning the microscope slides, and Katalin Parragné Derecskei and Barbara Dekan for their excellent technical assistance.

Author contributions

J.B. performed the experiments, analyzed the data and wrote the paper. S.T., O.D. and I.K. contributed to the in vivo experiments. J.T.Z. performed and analyzed the videomicroscopic measurements. H.O. participated in collection of human samples and data analysis. S.P., A.C., B.M. contributed to development of methodology and reviewed the manuscript. J.T. and Z.M. reviewed the manuscript. G.M.V., J.M., C.I. supervised and reviewed the clinical data. L.V. and B.D. designed and supervised the experiments, wrote and reviewed the paper. All authors read and approved the final manuscript.

Funding

J.B. was supported by OTKA-PD111656, B.D. by OTKA-KH130356, B.D. and V.L. by the Austrian Science Fund (FWF I3522, V.L.; FWF I3977 and I4677, B.D.), A.C. by OTKA 132225 ANN, and J.T. by the Hungarian Thematic Excellence Programme (TKP2020-NKA-26). JB and VL are recipients of János Bolyai Research Scholarship of the Hungarian Academy of Sciences, VL is supported by UNKP-19-4 New National Excellence Program of the Ministry for Innovation and Technology, and ZM by UNKP-20-3. We also thank Berta Kamprad Foundation, The Mats Paulsson Trust and The Stefan Paulsson Trust for their kind support.

Competing interests

The authors declare no competing interests.

Additional information

Supplementary Information The online version contains supplementary material available at <https://doi.org/10.1038/s41598-021-85162-0>.

Correspondence and requests for materials should be addressed to B.D. or V.L.

Reprints and permissions information is available at www.nature.com/reprints.

Publisher's note Springer Nature remains neutral with regard to jurisdictional claims in published maps and institutional affiliations.



Open Access This article is licensed under a Creative Commons Attribution 4.0 International License, which permits use, sharing, adaptation, distribution and reproduction in any medium or format, as long as you give appropriate credit to the original author(s) and the source, provide a link to the Creative Commons licence, and indicate if changes were made. The images or other third party material in this article are included in the article's Creative Commons licence, unless indicated otherwise in a credit line to the material. If material is not included in the article's Creative Commons licence and your intended use is not permitted by statutory regulation or exceeds the permitted use, you will need to obtain permission directly from the copyright holder. To view a copy of this licence, visit <http://creativecommons.org/licenses/by/4.0/>.

© The Author(s) 2021